

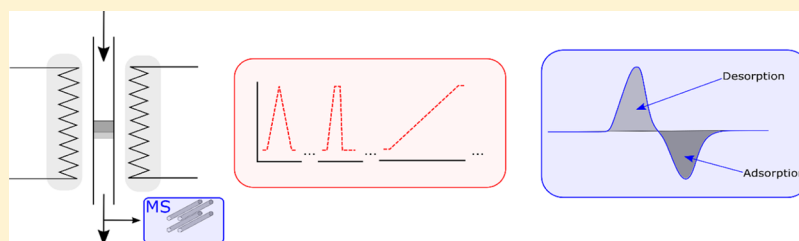
Fixed Feed Temperature-Programmed Modulation—A Quantitative Method To Obtain Thermophysical Parameters: Application to Chemical Warfare Agent Adsorbents

William T. Gibbons,[†] Scott Holdren,[‡] Junkai Hu,[‡] Bryan W. Eichhorn,[‡] and Michael R. Zachariah^{*,†,‡,§}

[†]Department of Chemical and Biomolecular Engineering and [‡]Department of Chemistry & Biochemistry, University of Maryland, College Park, Maryland 20742, United States

[§]Department of Chemical and Environmental Engineering, University of California, Riverside, Riverside 92507, California, United States

Supporting Information



ABSTRACT: Assessing the interaction between an adsorbate and a surface is essential for optimal engineering and design of adsorbents. For low-vapor-pressure adsorbates, which also exhibit relatively weak adsorption behavior (physisorption), both the sample and the system (manifolding, reactor, etc.) demonstrate similar affinities for the probe molecule. To minimize errors, researchers often use large sample masses, which are not often convenient to obtain, particularly for new lab-generated materials. To circumvent this issue, we demonstrate an approach where we fix the thermodynamic state of the system, and then thermally perturb a small sample under fixed feed conditions, thus eliminating the impact of the system response. By varying the thermal modulation rate, various regimes for analyzing adsorption, desorption, and reactions are possible, which enables the extraction of thermophysical parameters. In this paper, we first validate the fixed feed temperature-programmed modulation (FFTPM) method against a common adsorbate/adsorbent (methanol/BPL carbon) and then extend the technique to dimethyl methyl phosphonate (DMMP)/carbon systems. We demonstrate the utility of such an approach for quantitatively assessing adsorption capacities, differential heats of adsorption, isosteric heats of adsorption, and adsorption kinetics parameter estimation for DMMP on carbon adsorbents. The FFTPM method is well-suited for rapidly screening and characterizing adsorbents, reactive sorbents, and other systems which exhibit physisorption phenomena.

INTRODUCTION

Quantitative assessment of the adsorption behavior of weakly absorbing molecules is challenging but important, because many highly toxic nerve agents fall into this category. Designing adsorbents to capture such substances requires a reliable and quantifiable method for assessing the adsorption strength and capacity. Common adsorbent materials do not frequently possess both high adsorption strength and high capacity, making it difficult to permanently capture large quantities of adsorbate, necessitating an engineering tradeoff between adsorption capacity and adsorption strength. A common probe for adsorption capacity is dimethyl methyl phosphonate (DMMP), which is widely used as a less-toxic organophosphorus simulant for chemical warfare agents (CWAs) (e.g., sarin, soman, etc.).^{1–3} The phosphoryl group leads to strong intermolecular interactions between DMMP molecules, which results in the low vapor pressure and relatively large heat of vaporization of the liquid (77 Pa, 53.2 kJ/mol at 20 °C).⁴ The similarity between the phosphoryl

group of DMMP, and the phosphorous-flourine group present in many organophosphorus CWAs, is necessary to mimic the adsorption behavior of CWAs, but is difficult to manage experimentally, particularly if samples must be exposed to vapor phase DMMP over a range of concentrations. DMMP interacts with most system surfaces (tubing, sample holder, etc.) via physisorption, typically characterized as reversible surface/adsorbate interactions (lower than ~40 kJ/mol). Because the intermolecular interactions are on the same order as the adsorbate/surface interactions, a change in the vapor phase DMMP concentration will induce a time lag from the slow adsorption or desorption process as both the system and sample re-equilibrate with the new DMMP feed composition. For low-vapor-pressure adsorbates, such as DMMP, one observes very slow system equilibration, during

Received: September 13, 2018

Revised: March 25, 2019

Published: March 27, 2019

which the sample re-equilibrates. This serves to complicate studies of various adsorbents under DMMP feed conditions, because conventional dosing or loading methods are slow and often inaccurate. This inaccuracy arises because the sample response is muted by the system response, and de-coupling the two requires samples that adsorb large amounts of adsorbate relative to the system.

Conventional adsorption measurements may be broadly characterized as *static volumetric* or *gravimetric* techniques such as those used by standard surface area/porosity analyzer instruments and standard probe molecules including N₂, Ar, Kr, and other low-interacting well-behaved gases.⁵ Recently, water⁶ has been used as the probe molecule in the static volumetric technique with success near room temperature, but care must be exercised to ensure that the instrument operates isothermally and condensation (activity \approx 1.0) is avoided. Additionally, the concentration of water in each dose is relatively low ($P_{\text{sat}}(20\text{ }^{\circ}\text{C})_{\text{H}_2\text{O}} = 2.3\text{ kPa}$), requiring high sensitivity pressure transducers to accurately measure the uptake of water after dosing. Adsorbates with vapor pressures far lower than water (i.e., DMMP) would require high-resolution pressure transducers to detect small pressure changes on adsorption, or very large sample sizes, and thus the static volumetric technique is not suitable for DMMP adsorption measurements on reasonable timescales. Gravimetric adsorption techniques are more suitable for adsorption of low-vapor-pressure probe molecules, and often incorporate a temperature-controlled (heated and cooled) sample volume through which the adsorbate is introduced. The gravimetric system suffers from slow equilibration times, particularly when the adsorbate is “sticky” (low-vapor-pressure, relatively high heat of vaporization). When assessing DMMP adsorption, gravimetric methods are more suitable than volumetric methods, but adsorption equilibration periods in such systems have been reported to take days, weeks, and even months to reach completion, a factor compounded by the indirect exposure of the sample to adsorbate flow, which may result in large mass transfer resistance within the sample bed.⁷

Ideally, one would fix the thermodynamic state of the entire system (system + sample) and allow sufficient time for equilibration. Then perturb a very small portion of the system that contains the sample, while leaving the remainder of the system at equilibrium, thus avoiding the system lag induced by a change in the feed activity and the sample re-equilibration resulting from the activity change. We describe here a comprehensive method, fixed feed temperature-programmed modulation (FFTPM), that builds on previous efforts involving solid materials/sorbents in equilibrium with fixed probe molecule concentration(s). Previous work in this field included Foeth et al. who first described a TPD/MS method incorporating a fixed feed concentration with a packed bed reactor to assess the adsorption of CO₂ on to activated carbon. The authors applied various system models as well as the Langmuir adsorption model and estimated equilibrium adsorption quantities, heats of adsorption, and mass transfer effects from a series of measurements.⁸ Bianchi, Chafik, and others collaborated extensively to develop methods known as temperature-programmed adsorption equilibrium (TPAE) and adsorption equilibrium infrared spectroscopy (AEIR). Both methods incorporate a fixed feed concentration and linear temperature ramp along with IR and/or MS effluent concentration detection to estimate heats of adsorption and

adsorption isotherms for various adsorbate/adsorbent systems as well as conventional metal/metal oxide catalysts by fitting the experimental data to several adsorption models including Langmuir, Temkin, and Freundlich.^{9–12} These efforts have continued in earnest and the authors have successfully extended the TPAE and AEIR methods to assess the impact of superficial surface species (i.e., sulfates) as well as co-adsorbed species (i.e., water) on TiO₂-based catalysts for selective reduction of NO_x as demonstrated by the extensive work of Giraud and co-workers.^{13–15}

Our method presented here, FFTPM, is an extension to these previous works by slowly modulating the probe molecule concentration relative to the temperature modulation to effectively de-couple the system from the sample response, and thus enables a measurement of ads/desorption rates as well as characterization of thermodynamic parameters for “sticky” probe molecules including DMMP. FFTPM thus offers a useful lab-scale route to quantify ads/desorption of molecules that are difficult to manage via conventional approaches.

In this work, FFTPM is used to study the kinetic and thermodynamic parameters (adsorption isotherms, isosteric heats of adsorption) related to the adsorption and desorption of DMMP to/from different porous carbons. We first validate the FFTPM technique by measuring the thermodynamic parameters related to methanol adsorption on BPL carbon, a common activated carbon, and then comparing the results to literature values to demonstrate the applicability of FFTPM. We then apply FFTPM to study DMMP adsorption and desorption on both synthetic porous and BPL carbons. We demonstrate here that FFTPM is a very useful approach to evaluate physisorption of low-vapor-pressure, “sticky” adsorbates (e.g., DMMP), to extract important adsorption parameters such as isosteric heats of adsorption in a fraction of the time required by other methods. By simplifying and improving the data collection process, FFTPM facilitates the characterization of potential adsorbent materials, and is suitable for studying systems in which physisorption is the dominant process.

FFTPM Technique Background. When probe molecules have similar affinity for both the sample and the system (tubing, manifold, reactor, fittings, and related surfaces), as is typical for physisorbed species, it is difficult to de-couple the response of the system and the sample without employing a very large sample surface area relative to the system surface area. As an example, Kaplan studied DMMP adsorption on commercial activated carbon, which necessitated the use of large sample masses and large feed flow rates (15–25 g carbon, and up to 30 L/min) to measure breakthrough times of about several hours.¹⁶ This approach ensured that the sample surface area is orders of magnitude greater than the system surface area, and reduces the error contributed by the system to any measured parameter. Whereas the use of large volumetric flow rates is viable in most lab settings, the consistent synthesis of samples with masses of about \sim 10 g is generally not achievable. For the purposes of screening/characterizing new adsorbents synthesized at the lab scale, another method for eliminating the system response from the measurements is necessary. One such approach discussed here, FFTPM, ensures that the system remains at a steady state, whereas the sample is subjected to a change in temperature, and allows one to assess the adsorption characteristics of various engineered adsorbents with sample masses of \sim 10 mg.

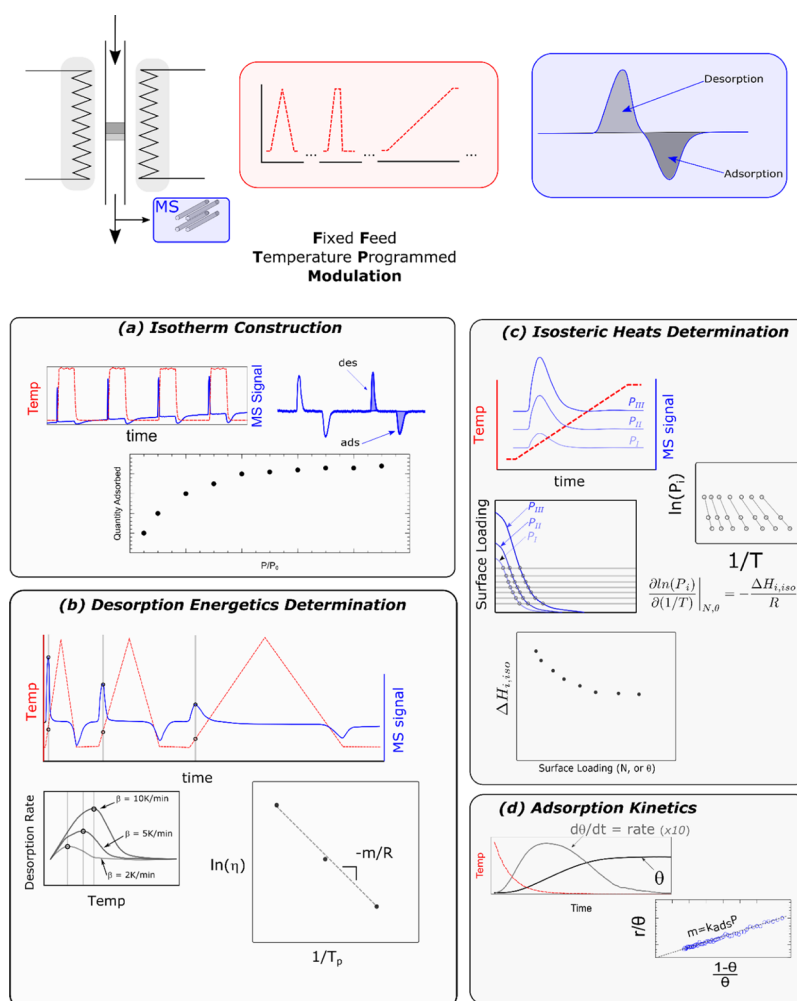


Figure 1. FFTPM technique for characterizing physisorption processes under fixed feed conditions with predominately molecular desorption. (a) Isotherm construction. (b) Implementation of TDS techniques to determine desorption energetics via variable heat rate method where η represents β/T_p or β/T_p^2 and m represents the heat of adsorption (ΔH) or the differential heat of adsorption (q_{diff}) at the sample coverage during the peak rate of desorption. (c) Isosteric heat determination via isobar construction under fixed feed, quasiequilibrium conditions; (d) adsorption kinetics determination via linearized Polanyi–Wigner (P – W) expression applied to the isothermal adsorption process upon sample cooling.

The basis of the FFTPM method is to ensure that the system of interest is at equilibrium before perturbation. For systems exhibiting primarily physisorption, with negligible reaction, we need to only consider the processes of adsorption and desorption. Characterization of both the adsorption and desorption processes is heavily dependent on the surface concentration or surface loading of the probe molecule. The dimensionless surface loading, θ , is commonly employed when deriving expressions related to adsorption, such as the Langmuir isotherm. We use the parameter θ preliminarily to build on the reader's familiarity with the common forms of expressions describing adsorption and desorption phenomena before establishing expressions relevant for FFTPM analysis. In practice, a precise quantitative estimation of θ is challenging, often requiring assumptions about the sorbent area accessible to the probe molecule as well as the molecular area and packing density.

Figure 1 provides an outline of the FFTPM technique to provide adsorbed quantities (Figure 1a), desorption energetics (Figure 1b), isosteric heats of adsorption (Figure 1c), and observed adsorption rates (Figure 1d). These measurements are discussed in greater depth in the following sections. The

basis of the FFTPM technique is to first fix the thermodynamic state of the system, and subsequently provide sufficient time for the system to equilibrate. Then, the system is pushed out of equilibrium, typically by heating with a linear temperature ramp, thus altering the balance of the adsorption and desorption processes, allowing for a quantitative assessment of the adsorbate loading as well as the desorption products. Rates of adsorption and desorption are initially in balance for a fixed feed condition at steady state, a condition verified by confirming a steady-state detector signal prior to heating. Upon application of a linear heating ramp, rates of adsorption and desorption are pushed out of equilibrium, with the rate of desorption exceeding the rate of adsorption, which results in a positive deviation in the detector signal. As heating continues, the exponential increase in the rate of desorption outpaces any change in the rate of adsorption, leading to a decrease in the adsorbate surface loading, and reaching a maximum rate of desorption that may be easily tracked by the detector. Under FFTPM conditions, the partial pressure of the probe molecule remains fixed in the reactor feed for the duration of the experiment, and thus the sorbent surface is undergoing a constant re-equilibration process during heating. For suffi-

sufficiently low heating rates, the surface will achieve a quasiequilibrium state as rates of adsorption and desorption are allowed enough time to equilibrate for each differential change in temperature. The impact of re-adsorption is thus a topic requiring further attention for FFTPM analyses, though re-adsorption is demonstrated to only impact the analysis of the desorption energetics.

With conventional thermal desorption spectroscopy (TDS) approaches, experimental conditions which minimize re-adsorption are nominally chosen.^{17,18} In the case of FFTPM, the feed is fixed, and the detector baseline offers a continuous material balance on the system (sample + adsorbate). One main strength of the FFTPM approach is that the sample is undergoing a continuous, nearly instantaneous, material balance, with adsorption events producing a negative deviation in the baseline, and desorption a positive baseline deviation. This response characteristic is made clear by considering an overall mass balance on the sample bed

$$\frac{dN_{i,(\text{bed})}}{dt} = \dot{N}_{i,\text{in}} - \dot{N}_{i,\text{out}} \quad (1)$$

For materials in which the primary mode of ads/desorption is molecular, rather than reactive/dissociative, when the flux of the probe molecule entering the bed is greater than the flux exiting, the derivative is positive, and the bed is accumulating the adsorbate. Conversely, when the rate of adsorption is greater than the rate of desorption, and the detector signal is below the previously established baseline. The rate of change of the effluent concentration as a function of time can be measured via any number of analytical methods (e.g., Fourier transform infrared spectroscopy¹⁹). The FFTPM technique may be simply extended to any number of detectors provided that the detector response is well characterized with respect to concentration of the species of interest. In our case, a mass spectrometer provides both qualitative and quantitative analysis of the effluent stream composition.

Temperature modulation is the key to this technique to obtain the desired information from the adsorbate/sorbent system under examination. For fast temperature modulation ($\sim 2\text{--}100\text{ }^\circ\text{C}/\text{min}$), we are not concerned with the sample equilibrium, but rather the total amount of material adsorbing or desorbing for a given feed activity (Figure 1b). For slow temperature modulation ($0.1\text{--}1.0\text{ }^\circ\text{C}/\text{min}$), we may safely assume quasiequilibrium during the modulation, because adsorption and desorption processes are provided enough time to maintain equilibrium and thermodynamic parameters such as heats of adsorption may be obtained, because the surface coverage is known as a function of time (and thus temperature). As noted previously, similar approaches have been employed by others, although the methods have not yet found widespread adoption. Herein, we present a similar approach to the TPAE method, denoted as FFTPM, to distinguish the different heat rate regimes as well as probe molecule pressure variation, which, when combined, allow the experimentalist to obtain the desired information. The main difference between TPAE and FFTPM is that the latter is not restricted to the maintenance of adsorption equilibrium, and thus, depending on the needs of the user, and the information of interest, one may select either a “fast” (no assumption of adsorption equilibrium) or “slow” (adsorption equilibrium is maintained) heat rate.

Isotherm Determination via FFTPM (Fast-Heating). If an isotherm describing the adsorption as a function of

adsorptive activity is desired, the total adsorbed material must be evaluated at a fixed activity. A rapid heat rate ($\sim 100\text{ }^\circ\text{C}/\text{min}$) is employed to drive the adsorbate fully off the surface in a short period of time, without heating to such a temperature that adsorbate/adsorbent decomposition occurs. This rapid heating increases the signal/noise ratio for the detector, simplifies integration, and shortens the time required to construct the isotherm. By limiting the maximum temperature to well below the point of carbon oxidation or decomposition,²⁰ we are able to rapidly and reversibly construct isotherms for the various adsorbate/adsorbent pairs. This process is depicted in Figure 1a. The adsorbate activity may be varied in steps of controllable amplitude and duration, or as a linear ramp as the changes in amplitude and duration become sufficiently small (as shown in Figure 2a). By

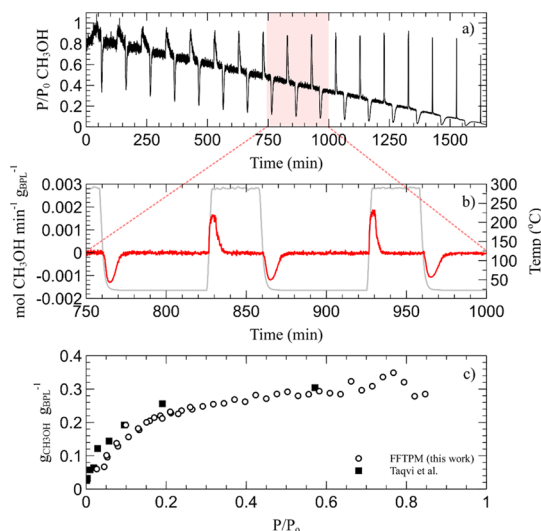


Figure 2. FFTPM fast-heating results for a methanol/BPL carbon system. (a) Methanol activity varied over 0.8–0.01, (decreasing at a rate of 3% per h) while a fast-heating temperature program is applied ($100\text{ }^\circ\text{C}/\text{min}$), (b) linear baseline subtraction employed to yield adsorption and desorption peaks free from impact of slowly decreasing methanol activity, and (c) results of adsorption and desorption peak integration compared to the work of Taqvi et al.

performing a linear baseline correction, the impact of a ramp in the feed activity may be subtracted (Figure 2b), provided that the changes in activity are very small relative to the changes induced by the des/adsorption processes. This approach is particularly useful for isotherm construction, during which the feed activity must vary over the desired range (typically 0.0–0.9 for FFTPM). Thus, the descriptor “fixed feed” is meant to describe a constant feed concentration for the duration of an individual desorption or adsorption peak. If the time (or temperature) at which a process or peak occurs is of interest, care by the user is also required to limit the change in feed concentration upon desorption, as large increases because of rapid desorption will induce subsequent transient system responses downstream of the reactor. Integration of the calibrated MS signal directly results in an adsorption capacity as a function of adsorbate activity (Figure 2c).

TDS via FFTPM (Fast-Heating). The FFTPM technique is not limited to a single application of TDS techniques, but one in particular, the variable heat rate method (depicted in Figure 1b), is applied here because of the experimental simplicity of the method, which involves comparing the “thermal desorption

spectra” at varied linear heating rates. TDS is a broad field and has been applied widely to a variety of systems, typically to chemisorbed species such as CO on metal surfaces.^{21–23} The heat of adsorption of chemisorbed species is often sufficiently high that desorption at low adsorbate partial pressures is negligible, and thus dosing is an effective approach to control surface loading. In the case of physisorption, desorption will occur at low adsorbate activities, and dosing is an ineffective method for dictating surface loading. Here, we employ a fixed feed activity along with traditional TDS approaches to demonstrate the viability of FFTPM for assessing physisorption energetics. The variable heat rate method for estimating the energetics of desorption is described briefly here, and in more detail in the [Supporting Information](#).

Subjecting an equilibrated sample to a linear heating rate yields an exponentially increasing rate of desorption, with the rate reaching a maximum as the surface concentration of the adsorbate is gradually depleted. The temperature at which the maximum desorption rate is achieved depends on factors including the initial surface loading, the desorption energy barrier, and the heating rate. Letting β represent the heating rate, we define the temperature at which the peak rate of desorption occurs as T_{peak} and recognizing that the first derivative of the desorption rate occurs at the same temperature regardless of the choice of surface concentration units, one can estimate the energetics of desorption from the relationship between heating rate and the temperature corresponding to the maximum rate of desorption. This approach is analogous to the work of Redhead,²⁵ with an extension to a flow reactor configuration experiencing re-adsorption. The work of Xia and Muhler et al.²⁴ offers an ideal starting point for the development of mathematical models describing desorption spectra for packed beds of porous materials to systems experiencing re-adsorption for both energetically homogeneous and energetically heterogeneous adsorbents. In their work, they discuss a series of characteristic groups (shown in eq 2) that are useful for assessing the impact of re-adsorption and indicating regimes in which the assumption of re-adsorption was minimal for both ideal and packed bed reactor configurations. The foundation of the FFTPM approach is a fixed feed pressure of the probe molecule, and thus, adsorption and/or re-adsorption of the probe molecule on to a recently vacated adsorption site is likely. To assess the impact of re-adsorption, under inert feed conditions, Xia et al. present a characteristic dimensionless group relating the product of the adsorption rate constant (k_a) and the partial pressure the adsorbate would exert if fully desorbed from the sorbent relative to the volumetric flow rate of inert feed gas as shown in eq 2. Under conditions of slow adsorption (small k_a), low adsorbent mass, and high volumetric flow, re-adsorption is not favored. Where k_a is the adsorption rate constant, $k_a = A_{\text{ads}} e^{(-E_{\text{ads}}/RT)}$, N_m is the number of moles of adsorbate on the sorbent, R is the ideal gas constant, T_a is the ambient temperature, and \dot{V} is the volumetric flow rate of the inert carrier gas.

$$(\text{re-adsorption negligible}) \ 1 \gg \frac{k_a N_m R T_a}{\dot{V}} \gg 1 \ (\text{re-adsorption favored}) \quad (2)$$

Interpreted another way, the characteristic group in eq 2 relates the potential for a probe molecule to undergo an adsorption event versus exiting the reactor, high values represent strong adsorption or large sample beds, and thus

favor re-adsorption. Adding a fixed concentration of the probe molecule to the feed serves only to increase the likelihood of re-adsorption and thus all FFTPM experiments will demonstrate larger values than those calculated via eq 2. Without prior knowledge of adsorption kinetics, the prudent approach is to assume that re-adsorption is present, particularly under high partial pressure fixed feed conditions. The subsequent analysis is moderately more complex, but does not introduce substantial error to the heats of adsorption estimation for systems exhibiting physisorption phenomena. If adsorption kinetics parameters are known with confidence, the experimental conditions remain the same, but the analysis may be simplified.

Our analysis of the FFTPM thermal desorption spectra, which includes the impact of re-adsorption, follows the work of Xia et al.,²⁴ and begins from the P–W expression,²⁵ for a first-order process

$$\beta \frac{d\theta}{dT} = A_{\text{ads}} e^{(-E_{\text{ads}}/RT)} P(1 - \theta) - A_{\text{des}} e^{(-E_{\text{des}}/RT)} \theta \quad (3)$$

where β is the heating rate, T is the absolute temperature, θ represents the surface coverage, P the partial pressure of the probe molecule, A the pre-exponential factor for adsorption or desorption, and E the activation energy barrier to adsorption or desorption.

The probe molecule partial pressure, P , is developed as follows

$$P = P_{\text{feed}} - \frac{N_m R T_a}{\dot{V}} \beta \frac{d\theta}{dT} \quad (4)$$

where the pressure of the probe molecule is estimated from the partial pressure entering the reactor and the amount of the probe molecule adsorbing or desorbing before exiting the reactor, under ideal gas conditions.

The partial pressure of the probe molecule begins at the feed concentration and then increases upon heating during the desorption process. Substitution of the expression for partial pressure into the P–W expression, subsequent expansion, substitution of expressions relating to energy barriers of ads/desorption and pre-exponential factors to enthalpy and entropy, respectively, and evaluation in the limit of $\frac{k_a N_m R T_a}{\dot{V}} \gg 1$ yield an equation similar to eq 14 in the work of Xia et al., with two additional temperature-independent terms, as shown in the [Supporting Information](#). These two additional terms are the direct result of the fixed feed pressure entering the reactor, P_{feed} and upon differentiation with respect to temperature, such that the change in surface coverage reaches a maximum at the corresponding peak temperature, T_p , that is $\frac{d^2\theta}{dT^2} = 0 @ T = T_p$, we obtain an expression identical to eq 16 (and also eq 42 in the case of re-adsorption for energetically heterogeneous systems) from the work of Xia et al.

This important result demonstrates that the breadth of desorption spectra analysis may not only be adapted to packed bed systems, but also to packed bed systems experiencing re-adsorption, such as those encountered during FFTPM experiments. One of the main results of Xia et al. is that for (first-order) energetically homogeneous systems under re-adsorption conditions, the enthalpy of adsorption (ΔH) may be determined from the slope of $\ln(\beta/T_p^2)$ versus $(1/T_p)$. For energetically heterogeneous systems, the differential heat of

adsorption (q_{diff}) may be determined from a plot of $\ln(\beta/T_p)$ versus $(1/T_p)$ as shown in eq 5 below.

$$\ln\left(\frac{\beta}{T_p}\right) = -\frac{q_p^{\text{diff}}}{RT_p} - \left[\frac{\Delta S^\circ}{R} + \ln\left(\frac{N_m RT_a}{p^\circ \dot{V}}\right) + \ln\left(\frac{q_p^{\text{diff}}}{\varepsilon_\delta}\right) \right] \quad (5)$$

In this study, we report q_{diff} because we see demonstrable surface heterogeneity under isosteric heat determination, particularly for BPL carbon. More information on the derivation of eq 5 can be found in the Supporting Information. The y -intercept contains information about the entropic changes upon adsorption. However, these parameters are outside the scope of our study and we will only be focused on the slope (q_{diff}) of $\ln(\beta/T_p)$ versus $(1/T_p)$ determined from our TDS analysis.

Isosteric Heat Determination via FFTPM (Slow-Heating). Under molecular ads/desorption conditions, the isosteric heat of adsorption (ΔH_{iso}), a useful engineering parameter, may be determined via a carefully constructed FFTPM slow-heating experiment consisting of an ~ 1 °C/min temperature ramp under quasiequilibrium conditions for a series of at least three adsorbate activities (Figure 1c). This parameter is useful for assessing surface “heterogeneity” or relative concentrations of adsorption sites across a spectrum of adsorption strengths, because the magnitude of the isosteric heat varies as a function of surface loading. The parameter is commonly used for engineering/design of adsorbent systems exhibiting large heat release/uptake upon adsorption/desorption and is often estimated by first constructing a series of adsorption isotherms at varying temperatures.^{26–28} The utility provided via FFTPM slow-heating is directly related to the long times and challenging experimental conditions required to construct adsorption isotherms using CWAs or CWA simulants such as DMMP. In such cases where the materials are toxic, difficult to manage experimentally, and/or difficult/unsafe to obtain/store in large quantities, the FFTPM slow-heating method provides a simple and thermodynamically consistent route to the isosteric heat determination. The isosteric heat determination via FFTPM slow-heating is described below.

To begin, the phase equilibrium between vapor (“v”) and adsorbed species (“a”) can be evaluated under ideal gas conditions, and low molar volumes of adsorbed DMMP through the Clausius–Clapeyron equation where the derivative is evaluated at constant surface loading (“N”)

$$\left(\frac{\partial \ln P}{\partial(1/T)}\right)_N = \frac{\Delta H^{\text{av}}}{R} \quad (6)$$

where R is the ideal gas constant, T is the absolute temperature, and P is the pressure of the adsorptive (DMMP in this case). Importantly, the enthalpy change ΔH^{av} , the isosteric heat of adsorption = $H^v - H^a$, represents the heat required to desorb the adsorbate at constant surface loading. Because it is experimentally difficult to perform calorimetric measurements at constant loading, the isosteric heat is difficult to measure directly, but straightforward to calculate from the isobars/isosteres constructed via the FFTPM approach. In this work, the notations ΔH^{av} and $\Delta H_{i,\text{iso}}$ are used interchangeably to represent the isosteric heat of adsorption of species i .

The FFTPM slow-heating method is ideally suited to measure $\Delta H_{\text{DMMP,iso}}$ because, by performing a slow-heating

step (1 °C/min) for a series of feed partial pressures, we may rapidly determine the relationship between the adsorbate loading and temperature. In such cases, it is essential that the heat rates be slow to ensure that the quasiequilibrium assumption holds, and the feed remain fixed to ensure a constant, or isobaric, adsorptive pressure. Rather than construct isotherms, we choose instead to construct isobars, due in large part to the ease and timeliness with which we may change the sample temperature while accurately determining the surface concentration. For example, in the case of DMMP/carbon adsorption, accurate isotherms require ca. 100 h to construct, resulting in large part from the relatively slow system equilibration. To construct multiple isotherms, three is generally considered the minimum number to determine $\Delta H_{i,\text{iso}}$, requires over 300 h. The same isosteric heats may be extracted from three FFTPM slow-heating experiments, requiring less than 10 h per experiment or a factor of 10 less time. Further, at no point in the analysis is an estimation of the monolayer capacity required. This does not preclude the estimation of the monolayer capacity, and subsequent assessment via various models for adsorption isotherms, but it is not required. Indeed, one of the primary failures of most adsorption models arises out of the assumption of a constant, or simply varying (e.g. linear, exponential, etc.) heat of adsorption as a function of surface concentration. Because real systems often do not exhibit such easily described characteristics, the models often fail to predict the adsorption behavior over a wide range of activities. As adsorbents grow in complexity and functionality, easily obtainable isosteric heats should prove valuable for informed engineering decision-making.

Adsorption Kinetics via FFTPM (Fast-Cooling). FFTPM may be employed to estimate the kinetic parameters related to adsorption processes. As discussed previously, in most of our experimental conditions the sample is in dynamic equilibrium, such that both the adsorption and desorption processes must always be taken into account. To obtain kinetic information the system must be pushed out of equilibrium and the rate of re-equilibration monitored. Under FFTPM conditions, this is most easily accomplished by first heating the sample to achieve complete desorption, and then rapidly cooling under fixed feed conditions at low probe molecule partial pressures so that re-adsorption is minimal. The isothermal temporal response may then be characterized via a linearized P–W expression. This approach is similar to the analysis presented by Xia and co-workers for a constant volume process,²⁹ but here the change in coverage as a function of time is monitored at a constant total pressure in a differential reactor.

The P–W expression for first-order processes may be written as

$$\frac{d\theta}{dt} = k_{\text{ads}}P(1 - \theta) - k_{\text{des}}\theta \quad (7)$$

Defining the net rate of change in coverage (positive for adsorption and negative for desorption) as $r = \frac{d\theta}{dt}$ and dividing by θ yields the linearized P–W expression

$$\frac{r}{\theta} = k_{\text{ads}}P\frac{(1 - \theta)}{\theta} - k_{\text{des}} \quad (8)$$

such that the adsorption rate constant $k_{\text{ads}}P$ is estimated from the slope of r/θ versus $(1 - \theta)/\theta$ over moderate changes in coverage.

In the case of the adsorption rate constant (k_{ads}) estimation, the user must use caution to avoid conditions under which internal mass transfer may impact the adsorption rate. At this juncture, the analysis of Trubitsyn and Vorontsov, who compared the relative rates of gas-phase diffusion of DMMP to transport within porous TiO_2 samples with 5 nm pores, offers a useful guide.³⁰ The condition of mass transfer limit may be assessed by comparing the rate of diffusion within the pores to the adsorption rate. FFTPM experiments are operated at high feed flow rates relative to the sample mass to eliminate concentration gradients within the sample bed as well as the impact of gas phase diffusion. Diffusion of the probe molecule within the pores of the porous materials under present conditions falls within the Knudsen diffusion regime because the pore diameter is several times smaller than the mean free path of the molecule, ~ 30 nm. The Knudsen diffusion coefficient (D_K) may be estimated with knowledge of the pore diameter (~ 1.7 – 3.6 nm) and pore length. The latter we estimate as being limited by the particle size $< 10 \mu\text{m}$. Then: $D_K = 97d_{\text{pore}}(T/M)^{0.5}$ and the characteristic pore diffusion time may be estimated as $= (d_{\text{particle}})^2/2D_K$. By comparing the maximum rate of adsorption, obtained in the limit of zero coverage, where $\frac{d\theta}{dt} = k_{\text{ads}}P$, we may assess whether the rate of diffusion within the pores is fast relative to the rate of adsorption.

Experimental Methods. Carbon (BPL, CMK-8, FDU-15)^{31–33} samples of known mass (10.0 ± 0.1 mg) were loaded into a quartz reactor of ID = 4.0 mm and OD = 6.0 mm. Samples were held in position by a plug of quartz wool, and sample temperature monitored via a downstream thermocouple as shown in Figure S1. Sample bed height varied proportionally with sample density, with a typical bed height of 2.0 mm to yield a sample volume of ca. 25 μL . Feed flow rates ranged from 25 to 100 sccm total, depending on the adsorbate concentrations used, with gas hourly space velocity values of 60 000–240 000 hr^{-1} , with typical conditions of 10 mg and 30 sccm total flow. Sample temperature was controlled and varied via a custom-built furnace, with low thermal mass and a heated zone of 40 mm, to minimize thermal gradients across the sample bed while simultaneously minimizing the heated volume of the system. Radial and axial temperature gradients are minimized by maintaining a small bed volume, and external mass transfer is minimized by maintaining high space velocities. Furnace temperature was controlled via a Eurotherm 91P PID controller, with an additional thermocouple located adjacent to the sample and outside the reactor. Bed temperatures were recorded via a separate thermocouple located at the trailing edge of the quartz wool plug.

Argon was used as a carrier gas and internal standard, with adsorbates (DMMP or methanol, Sigma-Aldrich >97%, used as received) added to the feed stream via temperature-controlled saturator cells described previously.³⁴ Saturator cell temperature control was achieved via custom-configured thermoelectric chillers fitted with a PID control, and temperatures were controlled within ± 0.1 $^\circ\text{C}$. Argon flow rates were set and monitored via Brooks 5850E mass flow controllers and a LabVIEW interface. Adsorption occurred at 22 $^\circ\text{C}$, whereas desorption occurred upon heating from 22 to 350 $^\circ\text{C}$, typically at a rate of 10 $^\circ\text{C}/\text{min}$, but ranging from 0.2 to 100 $^\circ\text{C}/\text{min}$

depending on experimental conditions and desired information. It is important to note, however, that for DMMP and methanol, desorption is complete well before 350 $^\circ\text{C}$. Typically, desorption is complete before the sample temperature reaches 150–200 $^\circ\text{C}$ for higher heat rates (> 10 $^\circ\text{C}/\text{min}$) and below 100 $^\circ\text{C}$ for slower heat rates (~ 1 $^\circ\text{C}/\text{min}$). The ramp to the maximum temperature was maintained to ensure a linear heat rate well after the desorption process was complete and the detector baseline returned to the previous steady-state value. The total heated volume of the system was 0.5 mL, and the surface area (quartz reactor and quartz wool) of the heated zone was 0.03 m^2 . Blank runs without a sample in the reactor showed that desorption from the heated volume of the system was minimal, of about the detection limit of the instrumentation, thus ensuring that changes in effluent signal were the result of adsorption on to, desorption from, and/or reaction on the sample rather than the reactor/system surfaces.

Online sample analysis was performed with an Extrel QPS1000 quadrupole mass spectrometer configured with a 19 mm quadrupole, 880 kHz quadrupole power supply, axial molecular beam electron ionization source with tungsten filaments (70 eV), and a pulse-counting electron multiplier detector with conversion dynode. A 50 μm , heated, fused silica inlet was used for sample introduction. The analysis was monitored, and ion intensities recorded, via Extrel's Questor5 Process Analysis Software.

The FFTPM approach was carried out for both methanol and DMMP adsorption on the carbons mentioned above. Methanol adsorption/desorption measurements were only performed on BPL carbon (see Figure 2) and used as a control to validate the FFTPM methodology by comparing our measured values against literature data collected by Taqvi et al.³⁵ The methanol adsorption/desorption procedure used slowly varying feed conditions (ca. 3%/h) to yield adsorption and desorption quantities over a range of activities, whereas the sample was subjected to fast-heating rates consisting of rapid changes in temperature followed by long dwell times to ensure complete adsorption or desorption. Methanol was introduced to the sample at 22 $^\circ\text{C}$, with an initial activity of 0.85, the activity was slowly reduced to 0.05 at 3%/h ($\sim 1\%$ change in feed activity per peak), before increasing again at the same rate. The temperature program began with a 1.0 h dwell at 22 $^\circ\text{C}$, a rapid ramp (100 $^\circ\text{C}/\text{min}$) to 300 $^\circ\text{C}$ (dwell 0.5 h), followed by a rapid cooling step (100 $^\circ\text{C}/\text{min}$) back to 22 $^\circ\text{C}$ (dwell 1.0 h). The temperature program looped continuously, yielding identical temperature profiles for each heating/cooling step. A linear baseline subtraction was applied to yield the net adsorption and desorption peaks, free from the impact of the activity ramp. These net ads/desorption peaks were then integrated to produce an adsorption isotherm. From the adsorption isotherm, the loading as a function of methanol pressure was obtained and compared against isotherms for similar systems in order to validate the technique. The FFTPM fast-heating method was then extended by varying the temperature ramp rates to produce a series of desorption peaks at a fixed activity with heating rates of 10, 5, and 2 $^\circ\text{C}/\text{min}$. These desorption peaks were subjected to the variable heating rate analysis to extract methanol desorption energies from BPL. Lastly, FFTPM slow-heating analysis was performed using the 1 $^\circ\text{C}/\text{min}$ heating step to extract isosteric heats of adsorption. Identical experiments to extract adsorption isotherms and isosteric heats of adsorption were performed

using DMMP as a probe molecule on BPL, CMK-8, and FDU-15 carbons.

Adsorption kinetics were estimated from a rapid cooling step under fixed feed conditions ($P_{\text{DMMP}} = 62 \text{ Pa}$, $P/P_0 = 0.8$). First, the carbon sample was heated to $300 \text{ }^\circ\text{C}$ (dwell 1.0 h), to ensure complete desorption of DMMP from the carbon sample. The sample was then cooled rapidly, reaching a stable, isothermal condition, after ca. 5 min. As the reactor nears ambient temperature, the cooling rate departs from the linear control, as a result of the vanishing temperature gradient between the reactor and the surroundings. Whereas adsorption occurs during cooling, sufficient time was provided to ensure only adsorption under isothermal conditions was employed for kinetic parameter estimation. The adsorption rate constant was estimated from the slope of the linearized P–W expression under the assumption that the surface coverage may be approximated as the ratio between the loading at a given time and the maximum loading (N_{max}) as defined previously.

RESULTS AND DISCUSSION

FFTPM Technique Validation—Adsorption Isotherm, Isothermic Heats, and Desorption Spectroscopy. The FFTPM methods were employed to produce an adsorption isotherm, estimate isothermic heats, and assess the energy barriers of desorption (q_{diff}) for a standard system (BPL carbon/methanol) as a validation of the technique. The feed concentration of methanol was set to decrease at a linear rate (3%/h), which produces a linear decrease in the methanol P/P_0 over time as seen by the steady decreases in the baseline in Figure 2a. When the temperature of the BPL carbon was modulated as described above ($\sim 100 \text{ }^\circ\text{C}/\text{min}$), the detected methanol P/P_0 increased relative to the decreasing baseline, which produces the sharp positive peaks shown in Figure 2a. The negative peaks (below the baseline) shown in Figure 2a correspond to the BPL adsorbing methanol as the carbon cools back down to room temperature. These positive and negative peak areas are a direct measurement of the amount of methanol adsorbed at each respective methanol activity (P/P_0). Qualitatively, we see that the positive peak (desorption) is broad and small at high methanol activities, consistent with the thermodynamic state of the system. The negative peaks (adsorption) are effectively a mirror image. Figure 2b shows a section of Figure 2a after a linear baseline correction is applied. Figure 2b also shows the reproducibility of the methanol adsorption/desorption process because the adsorption (negative) and desorption (positive) peaks have integrated peak areas within 1–2% in a methanol P/P_0 range of 0.1–0.8. The reversibility of the adsorption and desorption of methanol from BPL confirms that the interaction is occurring through physisorption. These integrated peak areas over the entire P/P_0 range are used to construct the adsorption isotherm presented in Figure 2c, where a comparison is made between our FFTPM fast-heating results and the work of Taqvi et al.³⁵

The overlaid methanol adsorption to/from BPL carbon demonstrates good agreement, with notable departure at low methanol activities, in the Henry's region of the isotherm. BPL carbon is a standard adsorbent and is commercially available but is not considered to be uniform between batches and manufacturers. The samples were produced commercially, but separated in time by approximately two decades, and thus, the reasonable agreement between methods is considered

sufficient to validate the FFTPM approach for producing adsorption isotherms.

The FFTPM measurements on the methanol/BPL system are extended to also estimate the differential heat of adsorption (q_{diff}) via the fast-heat rate approach as shown in Figure 3.

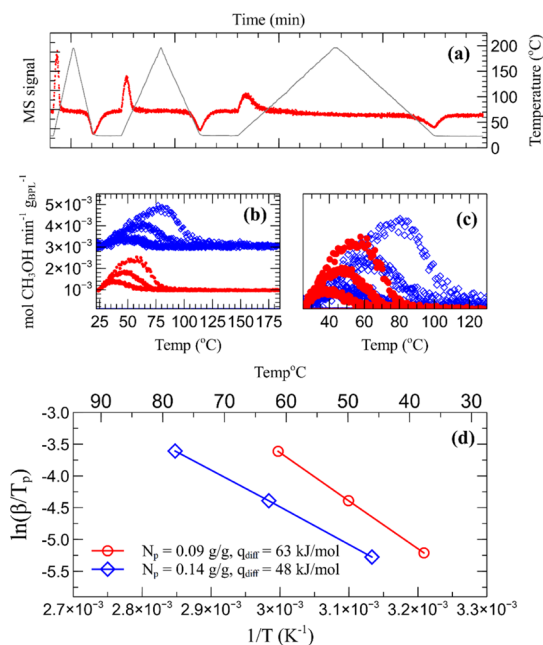


Figure 3. TDS via the variable heat rate method to assess the average desorption energy barrier for methanol from BPL carbon for an initial surface coverages of 0.2 (red) and 0.3 (blue) g/g. (a) Raw MS signal as a function of time and temperature demonstrating desorption and adsorption peaks, (b) calibrated MS signal as a function of temperature for two feed activities showing desorption peaks only, (c) baseline-subtracted desorption peaks for two activities [$P/P_0 = 0.2$ (red), 0.8 (blue)] and three heat rates (10, 5, 2 °C/min). (d) Linear fit of the heating rates as a function of the methanol desorption peak temperatures to extract the methanol desorption energetics (q_{diff} the differential heat of adsorption at the desorption peak).

Figure 3a presents the collected experimental data of the MS signal and temperature as a function of time. To extract the q_{diff} of methanol from BPL, the heating rate is varied (10, 5, and 2 °C/min) to produce different desorption peaks that reflect the desorption rate of methanol from BPL. Figure 3b,c are the desorption peaks obtained at varied methanol concentrations, which ultimately affect the initial methanol surface loadings on BPL (N_0), of 0.2 and 0.3 $\text{g}_{\text{methanol}}/\text{g}_{\text{BPL}}$, respectively. Figure 3d is constructed based on eq 2, β is the heating rate and T_{peak} is the temperature from the maxima of the methanol desorption peaks (shown in Figure 3c), plotted against $1/T_{\text{peak}}$. The slopes from these curves in Figure 3d are used to calculate the methanol desorption energy (q_{diff}) from BPL carbon at different surface loadings. The methanol differential heats of desorption are ~ 63 and 48 kJ/mol at surface loadings of $N_0 = 0.2$ and $0.3 \text{ g}_{\text{methanol}}/\text{g}_{\text{BPL}}$ and peak loadings of $N_p = 0.09$ and 0.14 g/g , respectively. From Figure 3d, the average energy barrier of methanol desorption decreases at larger methanol loading by approximately 15 kJ/mol . This is to be expected as higher loadings will tend toward liquid–liquid interactions compared to stronger van der Waals interactions between adsorbed methanol and the surface. At high methanol loading, apparently the q_{diff} of $\sim 48 \text{ kJ/mol}$ approaches the methanol

heat of vaporization (~ 38 kJ/mol), which suggests that the adsorbed methanol species exhibit interactions similar to liquid–liquid interactions. This is an expected result as molecular collisions tend toward methanol–methanol rather than methanol–surface at high loadings.

Lastly, we extended this work further to assess isosteric heats of adsorption for methanol on BPL via the FFTPM slow-heating rate approach (Figure 4). Figure 4a shows the amount

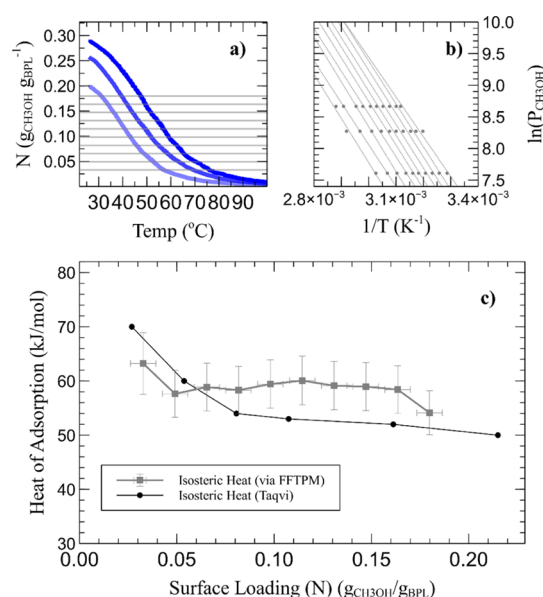


Figure 4. Isosteric heats for methanol adsorption on BPL carbon via the FFTPM slow-heating method compared to the work of Taqvi and co-workers, demonstrating the reasonable agreement between the two techniques, (a) three slow ramp rates for varied initial surface coverages shown as a function of absolute loading (N) with lines of constant loading indicated, (b) natural logarithm of the CH_3OH partial pressure in the feed stream vs inverse temperature for the loading vs temperature data given in (a,c) calculations of the isosteric heat of adsorption from the slopes of the lines in plot (b) as a function of surface loading.

of methanol adsorbed on BPL as a function of the temperature, which is used to construct the isobars shown in Figure 4b. The relationship shown in eq 6 allows us to extract the slopes of the various isobars to determine the methanol isosteric heats of adsorption on BPL as a function of the surface loading, which are compiled in Figure 4c. We compare our isosteric heats in Figure 4 with the results obtained by Taqvi et al. that were measured from four methanol adsorption isotherms at varied adsorption temperatures (25–100 °C). Although the techniques used to measure the isosteric heats of adsorption are different, the results show only small differences (at most ± 10 kJ/mol) in the isosteric heats for methanol on BPL. As the differences from the work done by Taqvi et al. are small, we attribute these differences to the differences between the BPL carbon batches and not the two techniques. This agreement with previous literature validates the FFTPM technique and allows us to reasonably extend this technique to unknown adsorbate/sorbent systems (i.e., DMMP and carbon).

DMMP Adsorption Isotherm on Carbons via FFTPM Fast-Heating. One of the main benefits of the FFTPM fast-heating method is that by selecting a series of desirable adsorbate activity values in sequence, allowing the system to reach equilibrium, and then recording the reactor effluent

composition upon thermal perturbation, one may produce an adsorption isotherm in relatively short time and with reasonable fidelity. As mentioned above, FFTPM measurements of methanol adsorption/desorption on BPL were used as a validation against results obtained by Taqvi et al. We repeated this procedure using DMMP on three different carbons (BPL, FDU-15, CMK-8) and the measured isotherms are shown in Figure 5. There are many differences between

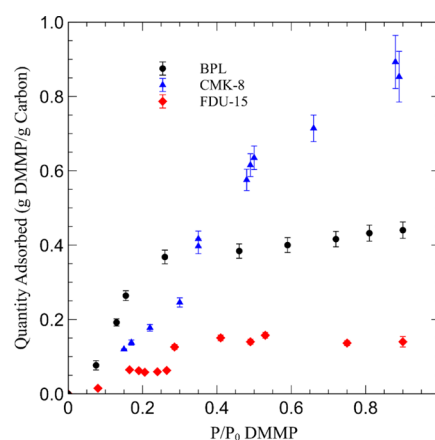


Figure 5. DMMP adsorption isotherms @ 295 K (22 °C) for carbon adsorbents (BPL, CMK-8, FDU-15).

these carbons including their pore sizes, pore volumes, and surface areas. In particular, BPL carbon is a microporous carbon with a primary pore size < 2 nm, whereas synthesized CMK-8 and FDU-15 are ordered mesoporous carbons (OMCs) that have uniform pore sizes of ~ 3.5 and 3.6 nm, respectively.³³ In addition, BPL carbon is known to contain mineral impurities such as Si, Al, S, Fe, Ca, Ti, and K,²⁰ whereas the synthesized OMCs are free of such impurities. These impurities found in BPL may play a role in how DMMP adsorbs and batch-to-batch variations in the impurities could contribute to scatter in measured heats of adsorption. More details of the characterization of these carbons can be found in our previous work.³³ Three different carbons were tested to investigate how DMMP interacts with synthesized OMCs compared to the commercial BPL carbon commonly found in gas filtration materials. From the measured DMMP isotherms in Figure 5, the BPL carbon demonstrates type I adsorption isotherm behavior, which is typical of microporous carbons. FDU-15 and CMK-8 carbons demonstrate type IV adsorption isotherms, which is characteristic of mesoporous/macroporous materials undergoing multilayer adsorption.⁵ Anecdotally, the DMMP and N_2 adsorption isotherms of the carbon samples are qualitatively quite similar to one another. Although the DMMP and N_2 isotherms exhibit similar shapes, in many cases, the probe molecule chosen for adsorption can have a significant effect on the resultant isotherm shape. For instance, Thommes et al. used water as a molecular probe in static volumetric and gravimetric systems to assess water adsorption and wetting behavior on various ordered carbons, and found that substantial water uptake does not occur until the water activity is > 0.4 for both CMK-8 and BPL.³⁶ Possibly, the similarities in the isotherms suggest that DMMP and N_2 undergo similar adsorption processes on the carbon sorbents.

Isosteric Heat of Adsorption of DMMP on Carbons via FFTPM Slow-Heating. FFTPM slow-heating was implemented to obtain the DMMP isosteric heats of

adsorption on BPL, FDU-15, and CMK-8, and are all shown in Figure 6. The isosteric heats of adsorption shown are obtained

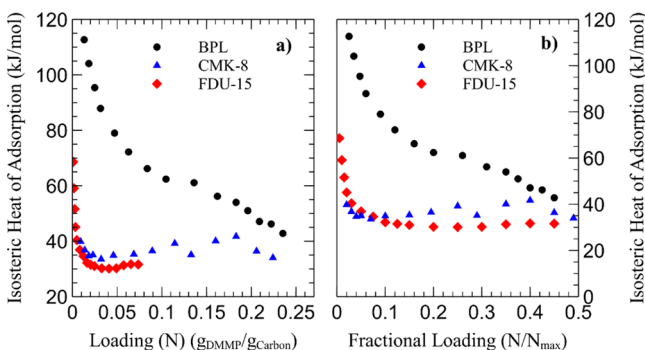


Figure 6. Isosteric heats of adsorption of DMMP on the different carbons tested. (a) Isosteric heats as a function of loading (N) and (b) as a function of fractional loading (N/N_{\max}).

in a similar manner that was described earlier for the methanol/BPL adsorbate/sorbent system (Figure 4). Similar to the methanol/BPL measurements, the amount of DMMP adsorbed as a function of temperature was plotted for the three carbons tested, and from the slope ($\ln(P_{\text{DMMP}})$ vs $1/T$) the isosteric heat of adsorption was determined at various surface loadings, as a function of N (Figure 6a), and N/N_{\max} (Figure 6b). The DMMP isosteric heat increases rapidly at low DMMP loadings ($N/N_{\max} < 0.1$) and is expected, because at low loadings, the initial sites where adsorbates will most strongly bind are preferentially occupied (i.e., low fractional coverage). Wilmsmeyer et al. discovered a similar finding measuring the desorption energy of DMMP from SiO_2 nanoparticles at various coverages.³⁷ Furthermore, apparently the isosteric heats of adsorption of DMMP on BPL are higher than those of the synthetic mesoporous carbons CMK-8 and FDU-15. This is likely a result of the minerals/metals (e.g., Si, Al, Fe, Ti) in BPL that may strengthen the adsorbate/adsorbent interactions. In addition, the lower average pore size of BPL (<1.7 nm) compared to FDU-15 and CMK-8 (3.5–3.6 nm) may also explain the larger isosteric heat of adsorption on BPL. DMMP adsorbed in the micropores of BPL may experience stronger capillary condensation effects compared to adsorption in the mesopores of FDU-15 and CMK-8. The capillary condensation of DMMP within the pores would suppress the vapor pressure of DMMP,³⁸ requiring more heat to desorb DMMP from these pores at a fixed loading (i.e., a higher isosteric heat of adsorption).

Using FFTPM to obtain the isosteric heat of adsorption is useful for adsorbent design for gas/solid interactions exhibiting physisorption phenomena and can be utilized to screen the efficacy of various sorbents for different gases (e.g., DMMP, methanol, water, hydrocarbons, etc.). The capability to extract isosteric heats of adsorption without measuring multiple adsorption isotherms or using calorimetry is advantageous for many types of systems. Lastly, we believe this technique can be applied to other heterogeneous adsorption and reactive sorbent systems, including systems demonstrating catalytic turnover and systems in which adsorbates undergo chemisorption or dissociative adsorption with isosteric heats of adsorption much larger than 50 kJ/mol. Under most conditions, the “real-time” material balance on the sample bed facilitated via the fixed feed approach is an asset rather than a hindrance.

Estimation of DMMP Adsorption Kinetics on Carbons via FFTPM Fast-Cooling.

FFTPM may be employed to estimate kinetic parameters related to adsorption processes, provided that the sample may be pushed far from equilibrium and the re-equilibration monitored as a function of time. This transient sample response may then be evaluated and related to kinetic parameters. In this work, we estimate the observed adsorption rate constant $k_{\text{ads,observed}}$ ($k_{\text{ads,obs}}$) for DMMP adsorption on to the carbon samples by first heating the samples until complete desorption has occurred, and then rapidly cooling the samples under a fixed feed ($P_{\text{DMMP}} = 62$ Pa). The label $k_{\text{ads,obs}}$ is used here to indicate that the reported adsorption rate constant is the rate constant observed for that specific experimental condition, and as a result may include effects of mass transfer and other resistances to adsorption. The isothermal temporal response is then characterized via a linearized P–W expression as discussed previously in the Background and Experimental Methods sections. Figure 7 provides the results of this fitting for the carbon samples over the coverage range of 0.4–0.75, well within the isothermal adsorption regime.

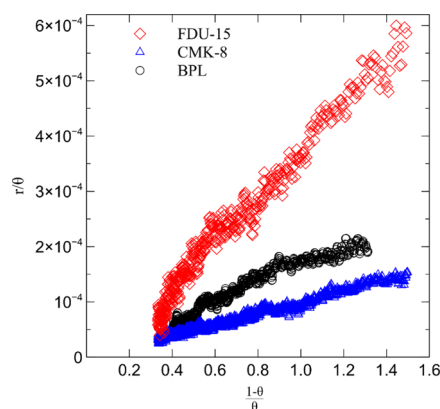


Figure 7. Linearized P–W transform of DMMP adsorption under fixed feed conditions ($P_{\text{DMMP}} = 62$ Pa) over the fractional coverage range ($\theta = N/N_{\max} = 0.4\text{--}0.75$). Adsorption kinetics ($k_{\text{ads,obs}}P$) are extracted from the slope of each fit and are presented in Table 1.

In Table 1, we can see that the characteristic time for diffusion within the pores is about 0.1 ms, which is 6–7 orders of magnitude smaller than the time required to reach a coverage of only $\theta = 0.1$ ($t_{0.1}$). This comparison suggests that the observed DMMP adsorption rate is significantly slower than the pore diffusion rate, and thus the entirety of the carbon sample is in dynamic equilibrium with the gas phase. As a result, we may assume that internal mass transfer effects do not strongly contribute to the estimation of the adsorption kinetic parameters. This analysis indicates that the FFTPM approach offers a route to kinetic parameter estimation via the observation and analysis of a transient response. Adsorption constants, in the form of $k_{\text{ads,obs}}$, are not widely reported for DMMP in the present literature. The $k_{\text{ads,obs}}$ values determined via FFTPM are similar to those reported by Xia et al. for CO adsorption on copper surfaces (10^{-4} to 10^{-6} $\text{Pa}^{-1} \text{s}^{-1}$),²⁴ suggesting that the values derived by FFTPM are within a reasonable range. In practice, the linearized P–W expression slope remains little changed over wide ranges of coverage, whereas the intercept is sensitive to the coverage range, and thus, we are unable to report $k_{\text{des,obs}}$ values with high

Table 1. Knudsen Diffusion Coefficient (D_{Knudsen}), Pore Diffusion Time ($T_{\text{pore diffusion}}$), Observed Adsorption Rate Constant ($k_{\text{ads,obs}}$), and Adsorption Time To Reach θ of 0.1 ($t_{0.1}$) for the Three Different Carbon Samples Undergoing DMMP Adsorption ($T = 22\text{ }^{\circ}\text{C}$, $P_{\text{DMMP}} = 62\text{ Pa}$) over the Fractional Coverage Range of 0.4–0.75

sample	d_{pore} (nm)	D_{Knudsen} ($\text{m}^2\text{ s}^{-1}$)	$t_{\text{pore diffusion}}$ (s^{-1})	$k_{\text{ads,obs}}$ ($\text{Pa}^{-1}\text{ s}^{-1}$)	R^2 (k_{ads} fit)	$t_{0.1}$
BPL	1.7	2.5×10^{-7}	$\sim 2 \times 10^{-4}$	2.8×10^{-6}	0.948	5.7×10^2
CMK-8	3.5	5.2×10^{-7}	$\sim 1 \times 10^{-4}$	1.6×10^{-6}	0.974	1.0×10^3
FDU-15	3.6	5.4×10^{-7}	$\sim 9 \times 10^{-5}$	6.9×10^{-6}	0.971	2.4×10^2

confidence. In order to address this deficiency, and to facilitate larger isothermal adsorption regions, future experiments should employ cooling via forced, rather than natural, convection, thereby reducing the time over which non-isothermal adsorption occurs while cooling. This improvement will enable FFTPM users to evaluate the linearized P–W expression at fractional coverages below 0.4, and allow for a more accurate determination of both observed rate parameters $k_{\text{ads,obs}}$ and $k_{\text{des,obs}}$ (and in turn the equilibrium constant K) from the rapid cooling step. In practice, this enables the user to obtain the adsorption isotherm as well as the observed adsorption kinetics from a set of experiments in which identical heating and cooling profiles are superimposed upon a slowly varying feed (as depicted in Figure 1a).

CONCLUSIONS

When assessing adsorption/desorption behavior for physisorbed, low-vapor-pressure, “sticky” adsorbates, one should keep in mind that the system and sample are tightly coupled. Because the probe molecule has a similar affinity for the system and the sample, detecting changes from solely the sample is difficult unless the system is maintained at equilibrium while the sample is perturbed. The FFTPM approach directly addresses this experimental challenge, and enables the determination of thermodynamic parameters relevant for rational adsorbent design. The FFTPM approach was harnessed to yield insight surrounding adsorption/desorption of the CWA simulant DMMP on BPL, CMK-8, and FDU-15 carbon adsorbents. This technique is well suited for rapid screening of various materials capable of high adsorption capacities as well as catalytic decomposition, and for developing the next generation of CWA adsorbents and catalysts. Synthetic carbons such as CMK-8 and FDU-15 do not provide heats of adsorption high enough to be used as CWA adsorbents, because the adsorbate does not interact strongly enough with the carbon surface to provide meaningful protection. The FFTPM approach allows the user to select appropriate feed and temperature modulation to yield the desired thermophysical properties for systems exhibiting primarily physisorption interactions. These properties include adsorption isotherms, desorption energy barriers, heats of adsorption, and adsorption kinetics. FFTPM is useful for timely screening and assessment of adsorbent/adsorbate pairs and may provide insight for applications such as dehumidification, adsorption chilling, volatile organics capture, and CWA capture/defeat.

ASSOCIATED CONTENT

Supporting Information

The Supporting Information is available free of charge on the ACS Publications website at DOI: 10.1021/acs.jpcc.8b08991.

Mass spectrometer calibration; test system configuration; and derivation of a variable heat rate method for desorption energetics’ determination via FFTPM (PDF)

AUTHOR INFORMATION

Corresponding Author

*E-mail: mrz@enr.ucr.edu.

ORCID

Michael R. Zachariah: 0000-0002-4115-3324

Notes

The authors declare no competing financial interest.

ACKNOWLEDGMENTS

We gratefully acknowledge the generous support of the U.S. Department of Defense through the Defense Threat Reduction Agency (HDTRA1-12-1-0005).

REFERENCES

- Wang, G.; Sharp, C.; Plonka, A. M.; Wang, Q.; Frenkel, A. I.; Guo, W.; Hill, C.; Smith, C.; Kollar, J.; Troya, D.; et al. Mechanism and Kinetics for Reaction of the Chemical Warfare Agent Simulant, DMMP(g), with Zirconium(IV) MOFs: An Ultrahigh-Vacuum and DFT Study. *J. Phys. Chem. C* **2017**, *121*, 11261–11272.
- Monji, M.; Ciora, R.; Liu, P. K. T.; Parsley, D.; Egoopoulos, F. N.; Tsotsis, T. T. Thermocatalytic Decomposition of Dimethyl Methylphosphonate (DMMP) in a Multi-Tubular, Flow-through Catalytic Membrane Reactor. *J. Membr. Sci.* **2015**, *482*, 42–48.
- Tušek, D.; Ašperger, D.; Bačić, I.; Čurković, L.; Macan, J. Environmentally Acceptable Sorbents of Chemical Warfare Agent Simulants. *J. Mater. Sci.* **2017**, *52*, 2591–2604.
- Butrow, A. B.; Buchanan, J. H.; Tevault, D. E. Vapor Pressure of Organophosphorus Nerve Agent Simulant Compounds. *J. Chem. Eng. Data* **2009**, *54*, 1876–1883.
- Thommes, M. Physical Adsorption Characterization of Nanoporous Materials. *Chem.-Ing.-Tech.* **2010**, *82*, 1059–1073.
- Nguyen, V. T.; Horikawa, T.; Do, D. D.; Nicholson, D. Water as a Potential Molecular Probe for Functional Groups on Carbon Surfaces. *Carbon* **2014**, *67*, 72–78.
- Saxena, A.; Singh, B.; Sharma, A.; Dubey, V.; Semwal, R. P.; Suryanarayana, M. V. S.; Rao, V. K.; Sekhar, K. Adsorption of Dimethyl Methylphosphonate on Metal Impregnated Carbons under Static Conditions. *J. Hazard. Mater.* **2006**, *134*, 104–111.
- Foeth, F.; Mugge, J.; Van Der Vaart, R.; Bosch, H.; Reith, T. Equilibrium Adsorption Data from Temperature-Programmed Desorption Experiments. *Adsorption* **1996**, *2*, 279–286.
- Hachimi, A.; Chafik, T.; Bianchi, D. Adsorption Models and Heat of Adsorption of Adsorbed Ortho Di-Methyl Benzene Species on Silica by Using Temperature Programmed Adsorption Equilibrium Methods. *Appl. Catal., A* **2008**, *335*, 220–229.
- Derrouiche, S.; Bianchi, D. Heats of Adsorption Using Temperature Programmed Adsorption Equilibrium: Application to the Adsorption of CO on Cu/Al₂O₃ and H₂ on Pt/Al₂O₃. *Langmuir* **2004**, *20*, 4489–4497.
- Couple, J.; Bianchi, D. Heats of adsorption of linear CO species adsorbed on reduced Fe/Al₂O₃ catalysts using the AEIR method in diffuse reflectance mode. *Appl. Catal., A* **2011**, *409–410*, 28–38.
- Dulaurent, O.; Bianchi, D. Adsorption isobars for CO on a Pt/Al₂O₃ catalyst at high temperatures using FTIR spectroscopy: isosteric heat of adsorption and adsorption model. *Appl. Catal., A* **2000**, *196*, 271–280.

- (13) Giraud, F.; Geantet, C.; Guillaume, N.; Gros, S.; Porcheron, L.; Kanniche, M.; Bianchi, D. Experimental Microkinetic Approach of De-NO_x by NH₃ on V₂O₅/WO₃/TiO₂ Catalysts. 1. Individual Heats of Adsorption of Adsorbed NH₃ Species on a Sulfate-Free TiO₂ Support Using Adsorption Isobars. *J. Phys. Chem. C* **2014**, *118*, 15664–15676.
- (14) Giraud, F.; Geantet, C.; Guillaume, N.; Loridant, S.; Gros, S.; Porcheron, L.; Kanniche, M.; Bianchi, D. Experimental Microkinetic Approach of De-NO_x by NH₃ on V₂O₅/WO₃/TiO₂ Catalysts. 2. Impact of Superficial Sulfate and/or V_xO_y Groups on the Heats of Adsorption of Adsorbed NH₃ Species. *J. Phys. Chem. C* **2014**, *118*, 15677–15692.
- (15) Giraud, F.; Couble, J.; Geantet, C.; Guillaume, N.; Loridant, S.; Gros, S.; Porcheron, L.; Kanniche, M.; Bianchi, D. Experimental Microkinetic Approach of De-NO_x by NH₃ on V₂O₅/WO₃/TiO₂ Catalysts. 6. NH₃-H₂O Coadsorption on TiO₂-Based Solids and Competitive Temkin Model. *J. Phys. Chem. C* **2018**, *122*, 24634–24651.
- (16) Kaplan, D.; Nir, I.; Shmueli, L. Effects of High Relative Humidity on the Dynamic Adsorption of Dimethyl Methylphosphonate (DMMP) on Activated Carbon. *Carbon* **2006**, *44*, 3247–3254.
- (17) Kanervo, J.; Keskitalo, T.; Slioor, R.; Krause, A. Temperature-Programmed Desorption as a Tool to Extract Quantitative Kinetic or Energetic Information for Porous Catalysts. *J. Catal.* **2006**, *238*, 382–393.
- (18) Kanervo, J. M.; Kouva, S.; Kanervo, K. J.; Kolvenbach, R.; Jentys, A.; Lercher, J. A. Prerequisites for Kinetic Modeling of TPD Data of Porous Catalysts-Exemplified by Toluene/H-ZSM-5 System. *Chem. Eng. Sci.* **2015**, *137*, 807–815.
- (19) Bianchi, D. A Contribution to the Experimental Microkinetic Approach of Gas/Solid Heterogeneous Catalysis: Measurement of the Individual Heats of Adsorption of Coadsorbed Species by Using the AEIR Method. *Catalysts* **2018**, *8*, 265.
- (20) Suzin, Y.; Buettner, L. C.; LeDuc, C. A. Behavior of Impregnated Activated Carbons Heated to the Point of Oxidation. *Carbon* **1998**, *36*, 1557–1566.
- (21) De Jong, A. M.; Niemantsverdriet, J. W. The Adsorption of CO on Rh(100): Reflection Absorption Infrared Spectroscopy, Low Energy Electron Diffraction, and Thermal Desorption Spectroscopy. *J. Chem. Phys.* **1994**, *101*, 10126–10133.
- (22) Collins, D. M.; Spicer, W. E. The adsorption of CO, O₂, and H₂ on Pt. *Surf. Sci.* **1977**, *69*, 85–113.
- (23) Redhead, P. A. Thermal Desorption of Gases. *Vacuum* **1962**, *12*, 203–211.
- (24) Xia, X.; Strunk, J.; Litvinov, S.; Muhler, M. Influence of Re-Adsorption and Surface Heterogeneity on the Microkinetic Analysis of Temperature-Programmed Desorption Experiments. *J. Phys. Chem. C* **2007**, *111*, 6000–6008.
- (25) King, D. A. Thermal Desorption from Metal Surfaces: A Review. *Surf. Sci.* **1975**, *47*, 384–402.
- (26) Srivastava, V. C.; Mall, I. D.; Mishra, I. M. Adsorption Thermodynamics and Isothermic Heat of Adsorption of Toxic Metal Ions onto Bagasse Fly Ash (BFA) and Rice Husk Ash (RHA). *Chem. Eng. J.* **2007**, *132*, 267–278.
- (27) Shen, D.; Bülow, M.; Siperstein, F.; Engelhard, M.; Myers, A. L. Comparison of Experimental Techniques for Measuring Isothermic Heat of Adsorption. *Adsorption* **2000**, *6*, 275–286.
- (28) Schmitz, B.; Müller, U.; Trukhan, N.; Schubert, M.; Férey, G.; Hirscher, M. Heat of Adsorption for Hydrogen in Microporous High-Surface-Area Materials. *ChemPhysChem* **2008**, *9*, 2181–2184.
- (29) Xia, X.; Naumann d'Alnoncourt, R.; Strunk, J.; Litvinov, S.; Muhler, M. Coverage-Dependent Kinetics and Thermodynamics of Carbon Monoxide Adsorption on a Ternary Copper Catalyst Derived from Static Adsorption Microcalorimetry. *J. Phys. Chem. B* **2006**, *110*, 8409–8415.
- (30) Trubitsyn, D. A.; Vorontsov, A. V. Experimental Study of Dimethyl Methylphosphonate Decomposition over Anatase TiO₂. *J. Phys. Chem. B* **2005**, *109*, 21884–21892.
- (31) Jun, S.; Joo, S. H.; Ryoo, R.; Kruk, M.; Jaroniec, M.; Liu, Z.; Ohsona, T.; Terasaki, O. Synthesis of New, Nanoporous Carbon with Hexagonally Ordered Mesostructure. *J. Am. Chem. Soc.* **2000**, *122*, 10712–10713.
- (32) Meng, Y.; Gu, D.; Zhang, F.; Shi, Y.; Yang, H.; Li, Z.; Yu, C.; Tu, B.; Zhao, D. Ordered Mesoporous Polymers and Homologous Carbon Frameworks: Amphiphilic Surfactant Templating and Direct Transformation. *Angew. Chem., Int. Ed.* **2005**, *44*, 7053–7059.
- (33) Huynh, K.; Holdren, S.; Hu, J.; Wang, L.; Zachariah, M. R.; Eichhorn, B. W. Dimethyl Methylphosphonate Adsorption Capacities and Desorption Energies on Ordered Mesoporous Carbons. *ACS Appl. Mater. Interfaces* **2017**, *9*, 40638–40644.
- (34) Butrow, A. B.; Buchanan, J. H.; Tevault, D. E. Vapor Pressure of Organophosphorus Nerve Agent Simulant Compounds. *J. Chem. Eng. Data* **2009**, *54*, 1876–1883.
- (35) Taqvi, S. M.; Appel, W. S.; LeVan, M. D. Coadsorption of Organic Compounds and Water Vapor on BPL Activated Carbon. 4. Methanol, Ethanol, Propanol, Butanol, and Modeling. *Ind. Eng. Chem. Res.* **1999**, *38*, 240–250.
- (36) Thommes, M.; Morell, J.; Cychosz, K. A.; Fröba, M. Combining Nitrogen, Argon, and Water Adsorption for Advanced Characterization of Ordered Mesoporous Carbons (CMKs) and Periodic Mesoporous Organosilicas (PMOs). *Langmuir* **2013**, *29*, 14893–14902.
- (37) Wilmsmeyer, A. R.; Uzarski, J.; Barrie, P. J.; Morris, J. R. Interactions and Binding Energies of Dimethyl Methylphosphonate and Dimethyl Chlorophosphate with Amorphous Silica. *Langmuir* **2012**, *28*, 10962–10967.
- (38) Gas Transport in Porous Media. In *Theory and Applications of Transport in Porous Media*; Ho, C. K., Webb, S. W., Eds.; Springer Netherlands, 2006; Vol. 20.